AD-A072 548 CALIFORNIA STATE UNIV LONG BEACH DEPT OF MECHANICAL --ETC F/G 20/4
PREDICTION OF UNSTEADY TURBULENT BOUNDARY LAYERS WITH FLOW REVE--ETC(U)
1979 T CEBECI, L W CARR, P BRADSHAW N00019-78-M-0466

UNCLASSIFIED NL

| OF |
AD
A072548

END
DATE
FILMED
9-79
DDC

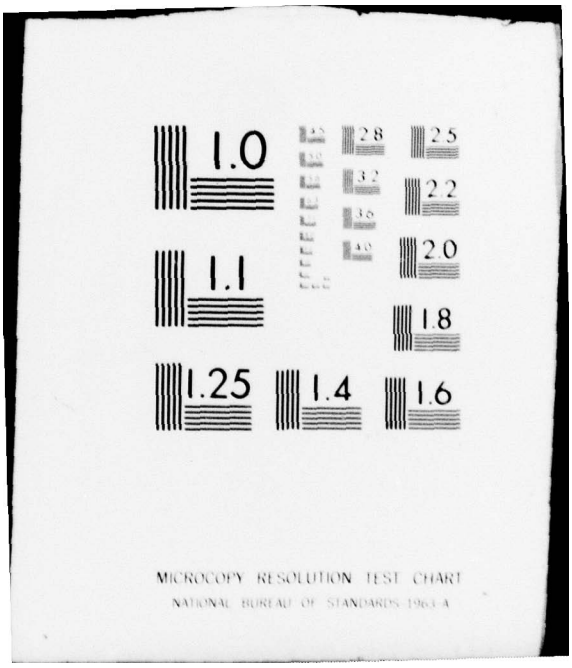
1.0
1.1
1.25
1.4
1.6
2.8
2.5
3.2
2.2
3.6
2.0
4.0
1.8
MICROCOPY RESOLUTION TEST CHART
NATIONAL BUREAU OF STANDARDS 1963-A

LEVEL II

# PREDICTION OF UNSTEADY TURBULENT BOUNDARY LAYERS WITH FLOW REVERSAL



Tuncer Cebeci
Professor of Mechanical Engineering
California State University at Long Beach, Ca 90840

Lawrence W. Carr
Research Scientist
U.S. Army, Aeromechanics Lab., Moffett Field, Ca 94035

Peter Bradshaw
Professor of Experimental Aerodynamics
Imperial College, London, England

Presented at the Second Symposium on Turbulent Shear Flows
July 2-4, 1979, Imperial College, London, England

N00014-78-M-0466

# PREDICTION OF UNSTEADY TURBULENT BOUNDARY LAYERS WITH FLOW REVERSAL*

Tuncer Cebeci
Professor of Mechanical Engineering, California State University at Long Beach, Ca. 90840

Lawrence W. Carr
Research Scientist, U.S. Army, Aeromechanics Lab., Moffett Field, Ca. 94035

Peter Bradshaw
Professor of Experimental Aerodynamics, Imperial College, London, England

## INTRODUCTION

The prediction of unsteady turbulent boundary layers with flow reversal is of importance in a number of aerodynamic problems, notably in dynamic stall, buffeting and gust studies. However, some of the more popular turbulence models implicitly assume that the wall shear is positive and their extension to unsteady flows with flow reversal is not easy. It requires a modification of the functional form of the law of the wall and the manner in which the wall shear is determined. Two near-wall assumptions are considered here. In the first, the near wall grid point is located in the logarithmic region and the law of the wall is used to link the flow properties at this grid point to the wall. In the second, a Van Driest formulation due to Cebeci and Smith (1) is used and implies that the grid point closest to the wall will occur in the viscous sublayer.

A further aspect of these flows of current interest is the possibility of a singularity occurring in the reversed-flow region. Examples of this phenomenon have also been reported in laminar flows but, in earlier studies two of us (Cebeci (2,3) and Bradshaw (4)) have shown that the occurrence is not a feature of the governing equations but is due to the limitations of the numerical procedure used. We shall demonstrate that, for the examples we study, there is no indicatation of such a singularity in turbulent flow either but there is a clear indication of rapid thickening of the boundary layer.

In addition to the examination of wall functions, we have also considered two turbulence models for unsteady flows without flow reversal. The algebraic eddy-viscosity formulation of Cebeci and Smith (CS) is compared with the transport model of Bradshaw, Ferriss and Atwell (5) (BF). Calculations were performed to determine whether the representation of unsteady flows with strong pressure gradients requires that account be taken of transport of turbulence quantities. As will be shown, the predictions with both models are nearly identical for steady flows but indicate significant differences with the increasing pressure gradient for unsteady flows.

In the following sections we describe the turbulence modelling, the governing equations, the numerical procedure and the results, respectively.

## TURBULENCE MODELLING

The Reynolds stresses are governed by the well-known transport equations whose left-hand sides are "substantial" derivatives of the Reynolds stresses – that is, the rate of change of Reynolds stress with respect to time as seen by an observer following the mean motion of the fluid substance. We write, for example

$$\frac{D(-\overline{u'v'})}{Dt} \equiv \left(\frac{\partial}{\partial t} + u\frac{\partial}{\partial x} + v\frac{\partial}{\partial y} + w\frac{\partial}{\partial z}\right)(-\overline{u'v'}) \qquad (1)$$

where in the case of an unsteady flow u,v and w are defined as ensemble averages over many repeats of the same experiment and are functions of time measured from the instant at which the unsteady flow is started. Here u' and v' are fluctuations about the ensemble-averages u and v, and are quasi-random functions of time (and spatial position) as usual, while $\overline{u'v'}$ is itself an ensemble average and thus a relatively smooth function of time. The right-hand sides of the Reynolds stress transport equations are exactly the same as in steady flow if the overbars are interpreted as ensemble averages. Therefore, the relative size of the time-derivative and space-derivative contributions to the left-hand side of the Reynolds stress transport equations is immaterial to a turbulence model based on term-by-term empirical approximation to the right-hand side of the Reynolds stress transport equations. All that matters is the size of $D\overline{u'v'}/Dt$ (hereafter referred to simply as "the rate of change of shear stress") as a whole. Therefore, the ability of a turbulence model to predict unsteady flows can be gauged by its ability to predict steady flows; commonly, turbulence models become less satisfactory when the rate of change of shear stress is large, because the empirical approximations on the right-hand sides are implicitly based on assumptions that the turbulence structure parameters change only slowly. Some calculation methods are implicitly based on the assumption that the rate of change of shear stress is itself small; examples include the eddy-viscosity assumptions used in some of the calculations presented below. Again, however, the potential of the method for predicting unsteady flows can be gauged from its ability to predict steady flows with rapid changes in the streamwise direction.

It is not possible to grade turbulence models for unsteady flow simply by the largest rate of change of shear stress – compared, say, to the major term $\overline{v'^2}\,\partial u/\partial y$ on the right-hand side of the equation – that they will reliably predict. This is because the frequency, as well as the magnitude of the time-dependent terms is important. Again, however, a unified analysis for steady and unsteady flow is

*This work was supported by the Naval Air Systems Command under contract N00019-78-M-0466.

possible; one need merely consider the ratio of the frequency seen by an observer following the mean motion of the fluid to the typical eddy frequency. First, consider steady flow with – say – streamwise periodicity of wavelength $\Lambda$ and typical mean speed U; the typical turbulence frequency could be written as $(-\overline{u'v'})^{1/2}/L$, where L is the length scale, and is of the same order as $\partial u/\partial y$ (equal to it if L happens to be equal to the mixing length $\ell$), while $\partial u/\partial y$ in the outer region of a boundary layer is of order $U/\delta$. The mean-flow frequency seen by the moving observer is $u/\Lambda$ and the ratio of this to the typical turbulence frequency is simply $\delta/\Lambda$. Therefore, if a turbulence model will adequately predict a steady streamwise-periodic flow with a given value of $\delta/\Lambda$, r say, the highest frequency of time-dependent, spatially-independent flow for which the model can be tested is r times the turbulence frequency (i.e. $r\,U/\delta$). One would expect r to be of order 0.1 at most. In a time-dependent flow with rapid spatial changes in the streamwise direction, the combined moving-axis frequency must be evaluated to apply the above criterion; note that in the important practical case of travelling-wave flows, the moving-axis frequency is small.

In summary, if both the rate of change of shear stress and the moving-axis frequency are no longer than the values the turbulence model can handle in steady flow, the model can be used with confidence and without change. No useful advice can currently be offered about turbulence models for unsteady flows with rapid changes. However, if the rapid changes are driven by strong pressure gradients, the Reynolds-stress gradients in the outer part of the boundary layer need not be calculated very accurately, while the inner layer is more tolerant of rapid changes because the typical turbulence frequency is high. It is unlikely that the "rapid distortion approximation" will be usable except in flows with extremely large time rates of change.

## GOVERNING EQUATIONS

The continuity and momentum equations can be written for two-dimensional unsteady incompressible laminar or turbulent thin shear layers as:

$$\frac{\partial u}{\partial x} + \frac{\partial v}{\partial y} = 0 \tag{2}$$

$$\frac{\partial u}{\partial t} + u\frac{\partial u}{\partial x} + v\frac{\partial u}{\partial y} = \frac{\partial u_e}{\partial t} + u_e\frac{\partial u_e}{\partial x} + \frac{\partial \tau}{\partial y} \tag{3}$$

Here

$$\tau = \nu\frac{\partial u}{\partial y} - \overline{u'v'} \tag{4}$$

and we recall that u' and v' denote fluctuations about the ensemble-average velocity; u' and v' are zero in unsteady laminar flow, and $\nu\,\partial u/\partial y$ is negligible outside the viscous sublayer in a turbulent flow. These equations are subject to the usual boundary conditions, which in the case of boundary layers are

$$y = 0 \quad u = v = 0; \quad y \to \delta \quad u \to u_e(x,t) \tag{5}$$

The presence of Reynolds stress term, $-\overline{u'v'}$ introduces an additional unknown to the system given by Eqs. (2) to (5). In this paper we present calculations using two different turbulence models. One is an algebraic eddy-viscosity formulation developed (for steady flows) by Cebeci and Smith and the other is a transport-equation model developed by Bradshaw, Ferriss and Atwell. In the CS model, we write Eq. (4) as

$$\tau = (\nu + \varepsilon_m)\frac{\partial u}{\partial y} \tag{6}$$

with two separate formulas for $\varepsilon_m$. In the so-called inner region of the boundary layer $(\varepsilon_m)_i$ is defined by the following formula:

$$(\varepsilon_m)_i = \{0.4y[1 - \exp(-y/A)]\}^2\left|\frac{\partial u}{\partial y}\right| \tag{7}$$

where

$$A = 26\nu u_\tau^{-1}[1 - 11.8(p_t^+ + p_x^+)]^{-1/2} \tag{8a}$$

$$u_\tau = \left(\frac{\tau_w}{\rho}\right)^{1/2}, \qquad p_t^+ = \frac{\nu}{u_\tau^3}\frac{\partial u_e}{\partial t}, \qquad p_x^+ = \frac{\nu u_e}{u_\tau^3}\frac{\partial u_e}{\partial x} \tag{8b}$$

In the outer region $\varepsilon_m$ is defined by the following formula

$$(\varepsilon_m)_o = 0.0168\int_0^\infty (u_e - u)dy \tag{9}$$

The inner and outer regions are established by the continuity of the eddy-viscosity formulas.

In the BF model, which is solved only outside the viscous sublayer, we assume $\tau = -\overline{u'v'}$ and write a single first-order partial-differential equation for it; the equation was originally developed from the turbulent energy equation but can be equally well regarded as an empirical closure of the exact shear-stress transport equation. It is

$$\frac{D\tau}{Dt} \equiv \frac{\partial \tau}{\partial t} + u\frac{\partial \tau}{\partial x} + v\frac{\partial \tau}{\partial y} = 2a_1\tau\frac{\partial u}{\partial y} - \frac{\partial}{\partial y}(\tau V_\tau) - 2a_1\frac{\tau^{3/2}}{L} \tag{10}$$

Here $a_1$ is a dimensionless quantity, $V_\tau$ is a velocity and L is the dissipation length parameter specified algebraically, as $L/\delta = f(\eta)$ with $\eta = y/\delta$ and $f(\eta)$ gives as an analytic fit to an empirical curve, by

$$f(\eta) = \begin{cases} 0.4\eta & \eta < 0.18 \\ 0.095 - 0.055(2\eta - 1)^2 & 0.18 \le \eta < 1.1 \\ 0.016\exp[-10(\eta - 1.1)] & \eta \ge 1.1 \end{cases} \tag{11}$$

In a more advanced version of this turbulence model (6) L itself is determined from a transport equation; we are now programming this version of the model for unsteady flow.

The turbulent transport velocity $V_\tau$, nominally $(\overline{p'u'} + \overline{u'v'^2})/\overline{u'v'}$ is proportional to a velocity scale of the large eddies and is chosen to be

$$V_\tau = 2a_1\frac{\tau_{max}}{u_e}g(\eta) \tag{12}$$

where $g(\eta)$ is

$$g = \begin{cases} 33.3n^2(0.184 + 0.832n) & n < 0.5 \\ 33.3n^3(0.368 + 2.496n^3) & 0.5 \le n < 1.0 \\ 18.7n + 14.60 & n \ge 1.0 \end{cases} \quad (13)$$

In the BF model equations, the inner boundary conditions for (2), (3) and (10) are applied outside the viscous sublayer, usually at $y_1 = 50\nu/u_\tau$. In the steady-flow study reported in (7), these boundary conditions are:

$$u_1 = u_\tau \left( \frac{1}{k} \ln \frac{y_1 u_\tau}{\nu} + 5.2 \right) \quad (14)$$

$$v_1 = - \frac{u_1 y_1}{u_\tau} \frac{\partial u_\tau}{\partial x} \quad (15)$$

$$\tau_1 = \tau_w + \frac{1}{\rho} \frac{\partial p}{\partial x} y_1 + \alpha^* \frac{\partial \tau_w}{\partial x} y_1 \quad (16)$$

Here $v_1$ is evaluated from the continuity equation (2), and $\alpha^*$ is evaluated from (2) and (3), on the assumption that the velocity $u$ is given by

$$\frac{u}{u_\tau} = \phi \left( \frac{u_\tau y}{\nu} \right) \quad (17)$$

for $0 < y < y_1$; Eq. (14) is, of course, a special case of (17). The evaluation of $\alpha^*$ is discussed in Ref. (7); the last term in (16) can be as large as half the second (pressure-gradient) term. In unsteady flow without flow reversal, we use the same inner "boundary" conditions at $y_1 = 50\nu/u_\tau$, but because of the presence of the time-dependent term in (3), $\alpha^*$ becomes more complicated. If we again assume that (17) holds — remember that the turbulence structure of the inner layer is unlikely to be affected unless the external-stream frequency is very high — as (2) and (3) give

$$\tau = \tau_w + \int_0^{y_1} \frac{\partial u}{\partial t} dy + \frac{\partial p}{\partial x} y_1 + \int_0^{y_1} \frac{\partial}{\partial x} (u^2) dy + uv \Big|_{y=y_1} \quad (18)$$

Integrating we can write

$$\tau = \tau_w + \frac{\partial}{\partial t} \int_0^{y_1} u dy - u(y_1) \frac{\partial y_1}{\partial t} + \frac{\partial}{\partial x} \int_0^{y_1} u^2 dy$$

$$- \cancel{u^2(y_1) \frac{\partial y_1}{\partial x}} - u(y_1) \frac{\partial}{\partial x} \int_0^{y_1} u dy + u^2(y_1) \frac{\partial y_1}{\partial x} \quad (19a)$$

because

$$\frac{\partial}{\partial x} \int_0^{y_1^+} \frac{u}{u_\tau} dy^+ \equiv 0$$

We can also write (19a) as

$$\tau = \tau_w + \frac{\partial p}{\partial x} y_1 + \nu \frac{\partial}{\partial t} \int_0^{y_1^+} \frac{u}{u_\tau} dy^+ + u_\tau F(y_1^+) \frac{\nu y_1^+}{u_\tau^2} \frac{\partial u_\tau}{\partial t}$$

$$+ \nu \frac{\partial u_\tau}{\partial x} \int_0^{y_1^+} \left( \frac{u}{u_\tau} \right)^2 dy^+ \quad (19b)$$

or as

$$\tau_1 = \tau_w + y_1 F \frac{\partial u_\tau}{\partial t} + \alpha^* y_1 \frac{\partial \tau_w}{\partial x} + \frac{\partial p}{\partial x} y_1 \quad (19c)$$

where $F = u/u_\tau$ at $y = y_1$ and $\alpha^*$ comes from the last term in (19b) and is the same as in steady flow.

Equation (19c) now replaces (16).

## SOLUTION PROCEDURE

We used Keller's two-point finite-difference method (called the Box method) to solve the system of equations described in the previous section. The application of this method to unsteady flows with no flow reversal using the CS model has been described in Ref. (8). Its application to steady two-dimensional flows using the BF model is described in Ref. (7). Here we present a brief description of its extension to unsteady two-dimensional turbulent flows with flow reversal. Due to the space limitations, we shall also limit the description to the equations that use the CS model. In a subsequent report, we hope to present a detailed description of the solution procedure for both model equations.

As in our previous studies, we transform the equations with

$$\bar{x} = x/L, \qquad \bar{t} = tu_0/L, \qquad \eta = (u_0/\nu\bar{x})^{\frac{1}{2}} y \quad (20a)$$

and a dimensionless stream function $f(\bar{x},\eta,\bar{t})$, where

$$\psi = (u_0 \nu x)^{\frac{1}{2}} f(\bar{x},\eta,\bar{t}) \quad (20b)$$

Here $u_0$ is a reference velocity, $L$ a reference length, and $\psi$ is the usual definition of stream function which satisfies the continuity equation (2). With the relations defined by (20) and with the definition of eddy viscosity, equations (2) to (4) and the boundary conditions can be written as

$$(bf'')' + \frac{1}{2} ff'' + m_3 = \bar{x} \left( f' \frac{\partial f'}{\partial \bar{x}} - f'' \frac{\partial f}{\partial \bar{x}} + \frac{\partial f'}{\partial \bar{t}} \right) \quad (21)$$

$$\eta = 0, \quad f = f' = 0; \quad \eta \to \eta_\infty, \quad f' = u_e/u_0 \equiv \bar{u}_e \quad (22)$$

Primes denote differentiation with respect to $\eta$ and

$$f' = u/u_0, \qquad m_3 = \bar{x} \left( \bar{u}_e \frac{\partial \bar{u}_e}{\partial \bar{x}} + \frac{\partial \bar{u}_e}{\partial \bar{t}} \right)$$

$$b = 1 + \epsilon_m^+, \qquad \epsilon_m^+ = \frac{\epsilon_m}{\nu} \quad (23)$$

For simplicity, we shall now drop the bars on $x$ and $t$.

## Standard Box Method

To solve (21) and (22) by the standard Box method, we first write (21) in terms of three first-order equations by introducing new dependent variables $u(x,\eta,t)$, $v(x,\eta,t)$, that is,

$$f' = u \tag{24a}$$

$$u' = v \tag{24b}$$

$$(bv)' + \frac{1}{2} fv + m_3 = x\left(u \frac{\partial u}{\partial x} - v \frac{\partial f}{\partial x} + \frac{\partial u}{\partial t}\right) \tag{24c}$$

We next consider the net cube shown in Fig. 1 and write difference approximations to (24) as discussed in several references (see, for example, Ref. (9)).

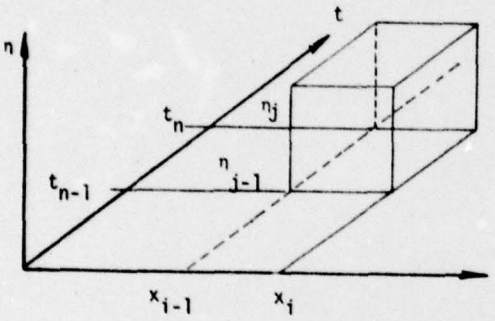


Fig. 1 Net cube for the standard Box method

Equations (24a) and (24b) are approximated using centered difference quotients and averaged about the midpoint $(x_i, t_n, \eta_{j-\frac{1}{2}})$. The difference quotients which are to approximate (24c) are written about the midpoint $(x_{i-\frac{1}{2}}, t_{n-\frac{1}{2}}, \eta_{j-\frac{1}{2}})$ of the cube whose mesh widths are $r_i, k_n$ and $h_j$. The resulting algebraic system, which is nonlinear, is linearized by Newton's method, and the linear system is solved by the block elimination method discussed in Ref. (9).

## Modified Box Method

When there is flow reversal across the boundary layer at some $x$ and $t$, we modify the standard Box method used for (24c) but retain that for (24a) and (24b) and center them at $(x_i, t_n, \eta_{j-\frac{1}{2}})$. To write the difference approximations for the Box centered at $(x_{i-\frac{1}{2}}, t_{n-\frac{1}{2}}, \eta_{j-\frac{1}{2}})$, we examine previously computed values of $u_{j-\frac{1}{2}}^{i-\frac{1}{2},n}$. If $u_{j-\frac{1}{2}}^{i,n} \geq 0$, then we use the standard Box method: if $u_{j-\frac{1}{2}}^{i,n} < 0$, then we write (24c) for the Box centered at P (see Fig. 2) using quantities centered at P, Q, and R, where

$$P \equiv (x_i, t_{n-\frac{1}{2}}, \eta_{j-\frac{1}{2}}), \qquad Q \equiv (x_{i-\frac{1}{2}}, t_n, \eta_{j-\frac{1}{2}}),$$

$$R \equiv (x_{i+\frac{1}{2}}, t_{n-1}, \eta_{j-\frac{1}{2}}) \tag{25}$$

Equation (24c) can then be written as

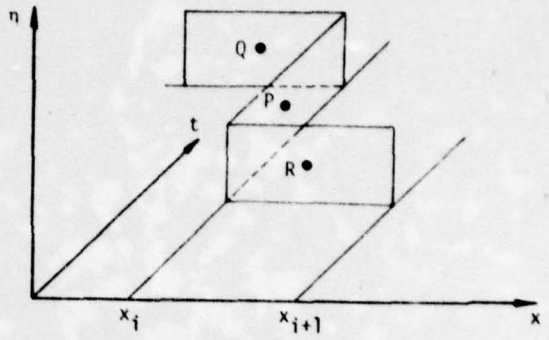


Fig. 2 Finite difference molecule for the zig-zag differencing

$$(bv)'(P) + \frac{1}{2}(fv)(P) = x(P)\Big[\theta u(Q)\frac{\partial u}{\partial x}(Q) + \phi u(R)\frac{\partial u}{\partial x}(R) - \theta v(Q)\frac{\partial f}{\partial x}(Q) - \phi v(R)\frac{\partial f}{\partial x}(R) + \frac{\partial u}{\partial t}(P)\Big] \tag{26}$$

Here

$$\theta \equiv \frac{x_{i+1} - x_i}{x_{i+1} - x_{i-1}}, \qquad \phi \equiv \frac{x_i - x_{i-1}}{x_{i+1} - x_{i-1}} \tag{27}$$

The resulting algebraic system is again nonlinear and its solution is obtained by using the procedure followed in the standard Box method.

## RESULTS AND DISCUSSION

To study the calculation of unsteady turbulent flows with flow reversal, we chose an external velocity distribution of the form

$$u_e = u_0[1 - \alpha(x - x^2)(t^2 - t^3)] \quad 0 < x < 1, \quad t > 0 \tag{28}$$

where $\alpha$ is a positive constant. The same velocity distribution was recently used by Cebeci (3) for laminar flows in order to study the computation of unsteady laminar flows with flow reversal using the solution procedure described earlier, and to see whether there is a singularity associated with such flows. Figure 3 shows the computed local skin-friction coefficient and Fig. 4 shows the corresponding results for displacement thickness in $0 < x < 1$ for various values of $t$ with $\alpha = 20$. It is clear from these results that the solution remains smooth for all calculated values of $t$, even when the region of reversed flow occupies the majority of the boundary layer and there is no hint of singularity. Instead, as in the study reported in Ref. (5), we see the familiar rapid Proudman-Johnson growth (10) of the boundary layer in the reversed flow region which, unless special measures are taken, terminates the calculations due to the rapid thickening of the boundary layer.

Figures 5 and 6 show the calculations for turbulent flows with $\alpha = 40$ and a unit Reynolds $u_0/\nu = 2.2 \times 10^6/m$. The results shown in Fig. 5 were obtained by using different expressions for A; those shown by circles were obtained by (8), and those shown by solid lines by writing (8) as

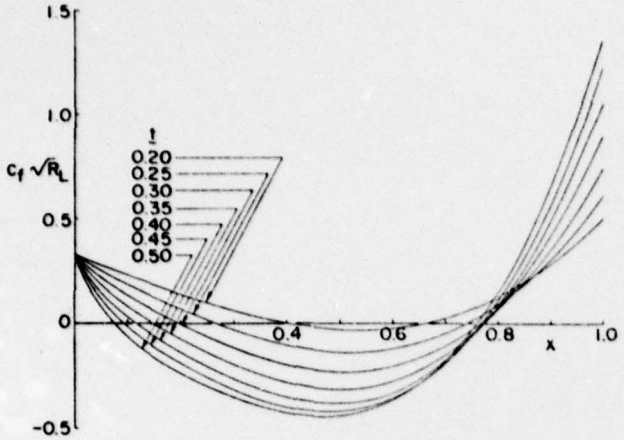


Fig. 3 Variation of local skin-friction coefficient $c_f\sqrt{R_L}$ with x for various values of t. Here $R_L = u_0 L/\nu$.

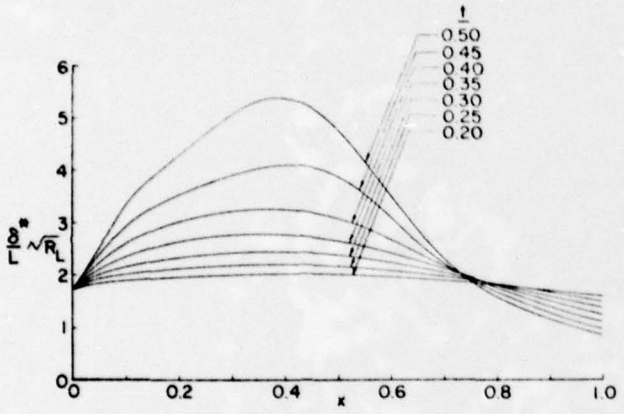


Fig. 4 Variation of dimensionless displacement thickness $\delta^*/L\sqrt{R_L}$ with x for various values of t.

$$A = 26\left(\frac{\tau}{\rho}\right)^{-1/2}_{max} \qquad (29)$$

As in seen, both expressions give nearly the same results.

The results in Fig. 6, as in laminar flows, indicate no signs of singularity for all calculated values of t. This is in contrast to the findings of Patel and Nash (11). Again we see the familiar rapid thickening of the boundary layer in the reversed flow region. If it were not for this, the calculations for greater values of t than those considered here, would have been computed.

Table 1 shows a comparison between $c_f$-values obtained by CS and BF models. At the present the calculations with the BF model have only been done for positive wall shear. For this reason, the comparisons in Table 1 are limited to those for which $\tau_w$ is positive.

As seen from the values in Table 1, the predictions of the CS and the BF models are nearly the same for steady flow. Initially the $c_f$ value at $x = 0$ calculated by the CS model is slightly lower than that computed by the BF model; this is due to matching. However, at some distance downstream, both methods give nearly the same answers. For unsteady flows,

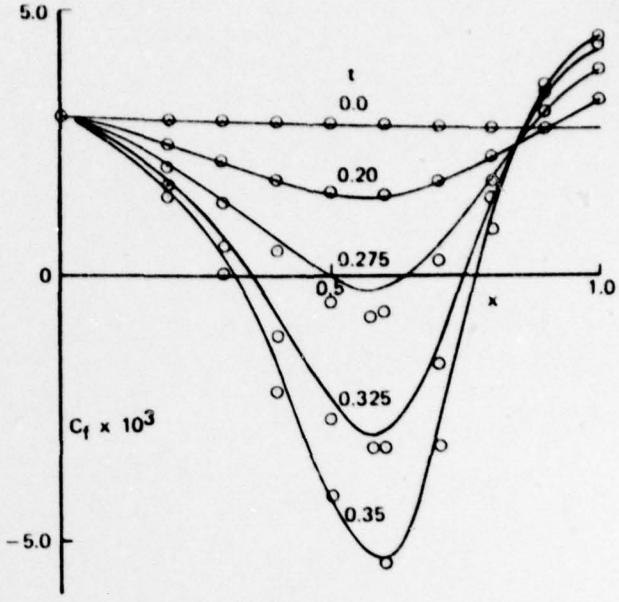


Fig. 5 Local skin-friction variation with x for various values of z. Solid lines denote the calculations made by (29) and circles by (8).

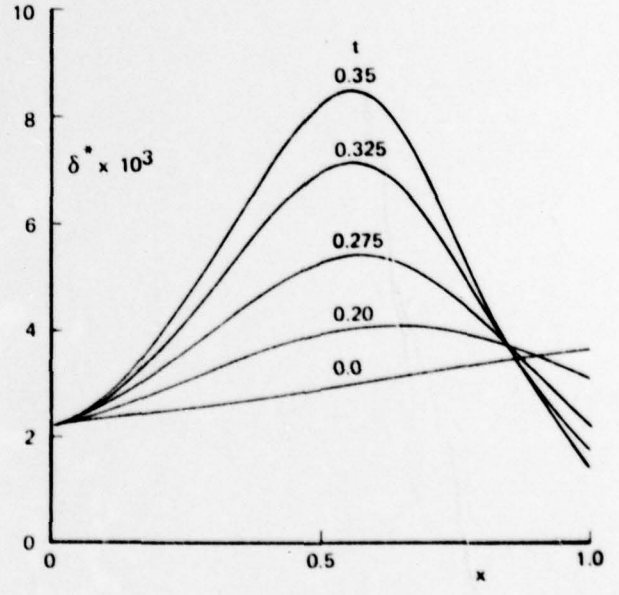


Fig. 6 Variation of displacement thickness with x for various values of t.

with pressure gradient increasing as a function of time and distance, the differences increase. Since the same numerical method is used in both cases, the difference may be attributed to the turbulence models. Additional studies are required to explain the predictions of each model but the differences may be due to the better ability of the transport model to cope with strong-pressure gradient flows.

Table 1 Computed $c_f$-values ($\times 10^3$) with CS and BF models

| | t = 0 | | t = 0.10 | | t = 0.225 | |
|---|---|---|---|---|---|---|
| x | CS | BF | CS | BF | CS | BF |
| 0 | 0.301 | 0.318 | 0.301 | 0.318 | 0.301 | 0.318 |
| 0.25 | 0.292 | 0.308 | 0.275 | 0.306 | 0.214 | 0.297 |
| 0.50 | 0.285 | 0.292 | 0.248 | 0.283 | 0.102 | 0.222 |
| 0.75 | 0.279 | 0.279 | 0.250 | 0.271 | 0.167 | 0.207 |
| 0.95 | 0.274 | 0.272 | 0.277 | 0.276 | 0.319 | 0.302 |

REFERENCES


1 Cebeci, T. and Smith, A.M.O., Analysis of Turbulent Boundary Layers, Academic Press, New York, 1974.

2 Cebeci, T., "The Laminar Boundary Layer on a Circular Cylinder Started Impulsively from Rest," to appear in Journal of Computational Physics, 1979.

3 Cebeci, T., "An Unsteady Laminar Boundary Layer with Separation and Reattachment," AIAA J., Vol. 16, No. 12, 1978, pp. 1305-1306.

4 Bradshaw, P., "Singularities in Unsteady Boundary Layers," to appear in AIAA J.

5 Bradshaw, P., Ferriss, D.H., and Atwell, N.P., "Calculation of Boundary-Layer Developments Using the Turbulent Energy Equation," J. Fluid Mech., Vol. 28, 1967, p. 593.

6 Bradshaw, P. and Unsworth, K., "Computation of Complex Turbulent Flows," in Reviews in Viscous Flows, Lockheed-Georgia Co. Rept. LG77ER0044, 1977

7 Cebeci, T., Chang, K.C. and Bradshaw, P., "Solution of a Hyperbolic System of Turbulence-Model Equations by the 'Box' Scheme," submitted for publication, 1979.

8 Cebeci, T. and Carr, L.W., "A Computer Program for Calculating Laminar and Turbulent Boundary Layers for Two-Dimensional Time-Dependent Flows," NASA TM 78470, 1978.

9 Cebeci, T. and Bradshaw, P., Momentum Transfer in Boundary Layers, McGraw-Hill/Hemisphere, Washington, D.C., 1977.

10 Proudman, I. and Johnson, K., "Boundary-Layer Growth Near a Rear Stagnation Point," J. of Fluid Mech., Vol. 14, 1962, pp. 161-168.

11 Patel, V.C. and Nash, J., "Unsteady Turbulent Boundary Layers with Flow Reversal," Unsteady Aerodynamics, Kinney, Ed., Vol. 1, 1975, p. 191.